

# ***Interactive comment on “Surface formation, preservation, and history of low-porosity crusts at the WAIS Divide site, West Antarctica” by John M. Fegyveresi et al.***

M. Schneebeli (Referee)

schneebeli@slf.ch

Received and published: 29 July 2016

The paper by Fegyveresi et al presents glaciological and meteorological observations concerning the formation of a thin crust at the snow surface around the WAIS drill site. The existence of this glazed crust has been described for several decades, but detailed information about the formation is lacking. This paper contributes to the understanding of the formation of these specific layers.

The methodology to investigate the formation of these layers is rather old-fashioned, and is not taking into account developments in snow characterization. The paper is in most aspects descriptive, with little quantitative information especially about the microstructure of the snow.

The paper describes in much detail the observations, but little quantitative data analysis and no modelling at all. The authors formulate extensively a general hypothesis on the formation of these layers, but do not substantiate their claims. The recent developments in snow metamorphism are not considered, and essential aspects in the interpretation are missing, especially concerning the radiation balance and the thermal conditions of the snowpack in the topmost layers of the snowpack.

I suggest the following revisions: - The short and longwave radiation balance should be calculated and used in the interpretation of the formation of the crusts. - Ideally, the weather data should be used to model the thermal conditions of the snowpack in the top 30 cm, this should not be a major difficulty (there are several snowpack models easily available, as Crocus and SNOWPACK). - A statistical analysis of the processes is needed, it does not become clear in the paper if the same weather conditions occur without formation of a glazed surface. - The hypotheses concerning the formation should be reformulated and quantified based on the results above

Based on the old-fashioned methods, several questions will probably remain open concerning the microstructural properties of the snow. It is a pity that now snow samples were cast using Diethyl-phthalate, this technique was already used in 1957 in Antarctica.

A general comment is also that the authors seem not to be aware of the difference between the terms "diagenesis" and "metamorphism". Diagenesis describes the densification by internal compaction or by a foreign sintering material. Metamorphism describes the recrystallization of minerals. Diagenetic processes in snow and firn occur in Antarctica below the isothermal zone (i.e. a few meters depth). Above, the dominant process is metamorphism. –

**Replaced terms to reflect metamorphism rather than diagenesis.**

**“We did correct all noted issues and responded to reviewer comments, specifically with the inclusion of more on the crust extent and on related snow pit studies (that were previously left out), although we did not add either additional modeling or a full energy balance study. The paper is already quite long, and we have specific challenges with attempting to incorporate either of these additional and lengthy studies. We are aware of the additional papers cited by the referees, and note the large amount of careful work involved. We do also hope to be able investigate further the possible effects of solar heating on the specific type of PRT sensors. We have added relevant citations to our paper. With our manuscript being this long and the difficulties with adding such large/expansive analyses, we believe it is better to write a phenomenological paper first and then address modeling and a full energy balance in a separate/future study.”**

Specific remarks:

l 38 According to instruments, these are radiation sensors, not insulation sensors

Reworded to "short and longwave radiation sensors"

l 40 There is no detailed data later in the manuscript about the crack spacing, so delete in abstract

Deleted

l 42 If this theory is correct, then a very strong convective vapor transport would be necessary, and calculations (see e.g. Ebner et al, Calonne et al.)

"Don't have a sufficient calculation here. We cannot partition accurately the relative contributions of vapor transport from below versus condensation of vapor in the atmosphere from other sources, but the wording 'may have contributed' should make this clear."

l 48 Was this layering also found in the snowpit?

It was and the detailed snow-pit investigation was added back to manuscript including text and 3 additional figures.

l 54 Are there any measurements done on the spatial extent of these layers (e.g. in the snowpit)?

"We have semi-quantitative measures, but not accurate maps, and we have additional calculations from occurrence of partial crusts in the core, which are well-quantified; a reference to that latter calculation can be found in the later-referenced PhD (Fegyveresi, 2015)."

l 110 The radiation instruments are described here in detail, but the data not used, why? These data are essential for the interpretation of crust formation. Especially snow surface temperature can be determined precisely from the pyrometers.

"They are used in the figures to show trends, but not used in more-detailed calculations. The final instrumentation was not the same from year-to-year; only in the final year was the full net radiometer installed. . .thus so a multi-year comparison of identical radiation data could not be performed."

l 165 I miss in this description the following information, resolved with mm-vertical resolution: density and specific surface area, ideally also coordination number. This information is available by a number of techniques, even with simple thick-sectioning of cast samples. Fig. 9 is just a photo with no quantitative information.

"Edited for clarity using snowpit data (See other new figures)."

l 170 Is there any statistics on size? This is very descriptive.

"No additional measured field statistics exist, however we added more detail for clarity. Also, related thesis chapter does include field observation data table with some additional observation notes on surface glazes (See Fegyveresi, 2015)"

l 201 How are the PRD-strings influenced by solar heating? The 10 cm depths is clearly not sufficient to prevent solar heating.

"As originally designed (see Muto et al., 2011), the sensor itself is housed inside a small aluminum tube, encased in glue. . .which minimizes direct solar heating. Still, we recognize that the very top surface sensors in this study (S0) that's placed under just a very small layer of snow is likely to be influenced slightly by some fraction of solar heating. Specific calibrations for this effect were not carried out in the field, but we felt the influence was likely minimal due to the nature of the sensor design and the "surface sensors" not being directly exposed to solar radiation."

l 204 A 3 K over 40 cm results only in a temperature gradient of 7.5 K m<sup>-1</sup>, far too small to create a relevant mass flux (see e.g. Pinzer et al, 2012).

Gradients steepen towards surface (See Alley et al., 1990 ; eg. Their figure 2). A 3k over 40 cm gradient likely has much steeper gradient near the surface. . .sufficient to drive the relevant mass flux.

1211 I would expect detailed drawings of the layer, how many snowpits measured, detailed statistics (spacing, size, ...)

Added back in the detailed pit maps and associated figures.

1217 How should I interpret "most commonly"? Any statistics here?

“As stated previously, 45% greater occurrence in Summers. Edited for clarity”

1221 I think you have either to reduce the approximate sign (and the about 2 m snow pit, or with the over a depth of 2.000 m?). What was the number of pits?

Stated previously – one snowpit per year for a 5 year period (so 5 pits)...but text has been added back in to clarify. Also, to clarify, all pits were measured to 2 meters, but due to sampling spacing and 5 cm thickness, the bottom sample was centered on 197.5 cm total depth (covering 195-200 cm).

1240 "should be quite accurate", what do mean in numbers by this?

“are well-constrained”

1249 The upper 30 cm are definitively not firm but snow, see the great discussion in Anderson, D. L., and C. S. Benson (1963), The densification and diagenesis of snow, in Ice and Snow: Properties, Processes and Applications, edited by W. D. Kingery, pp. 391–411, MIT Press.

Reworded to indicate that the upper portion of firm is generally considered snow.

1257 -274 The following descriptions are not a discussion, but a narrative of the observations

Relabeled the section “Synopsis and Discussion”

1275-282 I agree that surface hoar is an atmospheric deposition on the ground, but this paragraph disagrees with your hypothesis of vapor creeping out of cracks.

The paragraph states that there are two sources of hoar growth...from above and below. While some hoar growth was clearly related to high humidity fog episodes, the most dominant process related to hoar growth was sublimation related due to vapor transport

1283 Measured density data for crusts (for any snow layers) is not presented in this manuscript

Added in all snowpit density data and related figures. Also added text indicating all crusts densities measured and/or estimated over 400 kg m<sup>-3</sup>.

1301 I could not find any calculated temperature gradients in the result section

Would have to be related to modeling...need to calculate. TO DO

Referenced back to appropriate figures/data

Suggestions on recent papers on snow metamorphism

Calonne, N., F. Flin, C. Geindreau, B. Lesaffre, and S. Rolland du Roscoat (2014), Study of a temperature gradient metamorphism of snow from 3-D images: time evolution of microstructures, physical properties and their associated anisotropy, *The Cryosphere*, 8, 2255–2274, doi:10.5194/tc-8-2255-2014.

Ebner, P. P., C. Andreoli, M. Schneebeli, and A. Steinfeld (2015), Tomography-based characterization of ice-air interface dynamics of temperature gradient snow metamorphism under advective conditions, *Journal of Geophysical Research: Earth Surface*, 120(12), 2437–2451, doi:10.1002/2015JF003648.

Pinzer, B. R., M. Schneebeli, and T. U. Kaempfer (2012), Vapor flux and recrystallization during dry snow metamorphism under a steady temperature gradient as observed by time-lapse micro-tomography, *The Cryosphere*, 6(5), 1141–1155, doi:10.5194/tc-6-1141-2012.

# ***Interactive comment on “Surface formation, preservation, and history of low-porosity crusts at the WAIS Divide site, West Antarctica” by John M. Fegyveresi et al.***

Anonymous Referee #2

Received and published: 1 May 2017

Review of

Surface formation, preservation, and history of low-porosity crusts at the WAIS Divide site, West Antarctica.

By John M. Fegyveresi, Richard B. Alley, Atsuhiko Muto, Anaïs J. Orsi and Matthew K. Spencer

General

This is a comparatively comprehensive study of the formation of so-called surface crusts, involving daily observations of surface crust formation at the WAIS divide site in West Antarctica over five consecutive summers (2008/09 to 2012/13), including annual shallow snow-pit studies, snow temperature profiles and data (including shortwave radiation measurements) from an automatic weather station (AWS). The main conclusion is that crusts form most commonly in the summer from the effects of a large daily temperature cycle. There also appears to be crust formation in winter, as yet for unknown reasons.

The paper provides useful and original data for model development and evaluation, and the topic is suitable for publication in TC. The paper is rather descriptive, but useful, as the authors state in line 275: “Our data provide strong constraints on models of many of the observed processes.” However, the value of the study and analysis would be greatly quantified if the AWS and snow temperature data were used to calculate the surface energy balance, see comments below. I recommend to do this, which will require major revisions.

"We did correct all noted issues and responded to reviewer comments, specifically with the inclusion of more on the crust extent and on related snow pit studies (that were previously left out), although we did not add either additional modeling or a full energy balance study. The paper is already quite long, and we have specific challenges with attempting to incorporate either of these additional and lengthy studies. We are aware of the additional papers cited by the referees, and note the large amount of careful work involved. We do also hope to be able investigate further the possible effects of solar heating on the specific type of PRT sensors. We have added relevant citations to our paper. With our manuscript being this long and the difficulties with adding such large/expansive analyses, we believe it is better to write a phenomenological paper first and then address modeling and a full energy balance in a separate/future study."

Major comments

While explicit modelling of microphysical snow processes is beyond this MS's scope, a more quantitative interpretation can be achieved relatively easily by using the AWS and snow temperature data to close the surface energy balance. This will greatly aid the discussion by quantifying the sign and magnitude of surface energy fluxes, including the transport of water vapour by sublimation/deposition, during episodes of crust formation. See e.g. Van As and others (2005; 2006).

l. 45: “often warmed the near-surface snow above the air temperature, contributing to mass transfer. . .” This suggests that temperature gradient is a sufficient condition for sublimation, but this requires a specific humidity gradient (a less stringent condition. The relative humidity in the air may be below saturation; that in the snow is likely to be much closer to saturation because of proximity to the moisture source in the snow. So temperature gradient really is enough.

"We reworded for clarity."

I. 118: Were relative humidity measurements corrected for low-temperature offsets (See Andersen and others, 1994)?

"They were. All humidity values shown are corrected and represented in terms of saturation vapor pressure over ice (as described by Anderson 1994)"

I. 152: "accumulation at the site is relatively evenly distributed through the year, justifying this approximation"; this may be true for the climatological precipitation, but is there quantitative support that this holds for individual years as well?

"We added back the more-detailed pit study (including 3 figures) to help better illustrate/quantify this."

I. 201: "following the air temperatures as expected". Figure 10: Surface energy balance considerations dictate that the amplitude of the daily cycle in surface temperature exceeds that in air temperature, to allow for nocturnal cooling and daytime heating by sensible heat exchange. This appears not to be the case in these time series. Please comment.

"It is accurate that if sensible heat transfer is occurring, the temperature must be as the reviewer states; however there is no guarantee that sensible heat transfer is occurring. We edited wording and identified specific sensors for clarity."

Figure 13: please translate y-axis into average crusts per individual month, and include standard deviation as error bar. Mention ice core time interval in caption.

"Adjusted figure to show an inset showing average crusts per month with 1 sigma stdev."

Minor/Textual comments

I. 38: "insolation sensors" refers to incoming shortwave radiation. Better: "shortwave radiation sensors". "Insolation sensors" was used as there were both short and longwave sensors used. . .depending on the year.

"We adjusted text to "short and longwave radiation sensors"."

I. 113: pyrogeometers -> pyrgeometers .

"Corrected"

I. 191: crust removal -> hoar removal (?)

"Correct. Adjusted text to read "hoar"."

I. 330: "warm and windy air masses" an air mass cannot be windy, please reformulate.

"Reworded to "Such warm air masses paired with these high winds,""

References Anderson, P., 1994: A method for rescaling humidity sensors at temperatures well below freezing, J. Atmos. Oceanic Technol. 11, 1388-1391. (Added) Van As, D. and M. R. van den Broeke, 2006: Structure and dynamics of the summertime atmospheric boundary layer over the Antarctic plateau, II: Heat, momentum and moisture budgets, J. Geophys. Res. 111, D007103, doi:10.1029/2005JD006956. Van As, D., M. R. van den Broeke, R. S. W. van de Wal, 2005: Daily cycle of the surface layer and energy balance on the high Antarctic plateau, Antarctic Science 17, 121-133.

1 **Surface formation, preservation, and history of low-porosity crusts at the**  
2 **WAIS Divide site, West Antarctica.**

3 John M. Fegyveresi<sup>1,2</sup>, Richard B. Alley<sup>2</sup>, Atsuhiko Muto<sup>3</sup>, Anais J. Orsi<sup>4</sup>,  
4 Matthew K. Spencer<sup>5</sup>

5  
6 <sup>1</sup>Terrestrial and Cryospheric Sciences Branch, U.S. Cold Regions Research and  
7 Engineering Laboratory (CRREL), Hanover, NH, 03755, USA.

8  
9 <sup>2</sup>Dept. of Geosciences, and Earth and Environmental Systems Institute, Pennsylvania  
10 State University, University Park, PA, 16802, USA.

11  
12 <sup>3</sup>Dept. of Earth and Environmental Science, College of Science and Technology, Temple  
13 University, Philadelphia, PA, 19122, USA.

14  
15 <sup>4</sup>Laboratoire des Sciences du Climat et de l'Environnement, LSCE/IPSL, CEA-CNRS-  
16 UVSQ, Université Paris-Saclay, F-91191, Gif-sur-Yvette, France.

17  
18 <sup>5</sup>School of Physical Sciences, Lake Superior State University, Sault Sainte Marie, MI,  
19 49783, USA.

20

21

22 *Correspondence to:*

23 J. M. Fegyveresi ([fegy.john@gmail.com](mailto:fegy.john@gmail.com); john.m.fegyveresi@usace.army.mil)

24 **Key Words:**

- 25 • Antarctic snow surface, ice cores, field observations, snow-surface crusts, bubble-  
26 free layers, vapor transport, firn properties, snow physics.

27

28

29

30

31

32

### Abstract

33 Observations at the WAIS Divide site show that near-surface snow is strongly altered by  
34 weather-related processes such as strong winds and temperature fluctuations, producing features  
35 that are recognizable in the deep ice core. Prominent “glazed” surface crusts develop frequently at  
36 the site during summer seasons. Surface, snow pit, and ice core observations made in this study  
37 during summer field seasons from 2008-09 to 2012-13, supplemented by Automated Weather  
38 Station (AWS) data with ~~insolation-short and longwave radiation~~ sensors, revealed that such  
39 crusts formed during relatively low-wind, low-humidity, clear-sky periods with intense daytime  
40 sunshine. After formation, such glazed surfaces typically developed cracks in a polygonal pattern  
41 ~~with few meter spacing,~~ likely from thermal contraction at night. Cracking was commonest when  
42 several clear days occurred in succession, and was generally followed by surface hoar growth;  
43 vapor escaping through the cracks during sunny days may have contributed to the high humidity  
44 that favored nighttime formation of surface hoar. Temperature and radiation observations showed  
45 that daytime solar heating often warmed the near-surface snow above the air temperature, which  
46 we infer produced a specific humidity gradient contributing to mass transfer, the air temperature,  
47 ~~contributing to mass transfer~~ favoring crust formation and then surface hoar formation.  
48 Subsequent investigation of the WDC06A deep ice core revealed that crusts are preserved  
49 through the bubbly ice, and some occur in snow accumulated during winters, although not as  
50 commonly as in summertime deposits. Although no one has been on site to observe crust  
51 formation during winter, it may be favored by greater wintertime wind-packing from stronger  
52 peak winds, high temperatures and steep temperature gradients from rapid midwinter warmings  
53 reaching as high as -15°C, and perhaps longer intervals of surface stability. Time-variations in  
54 crust occurrence in the core may provide paleoclimatic information, although additional studies

55 are required. Discontinuity and cracking of crusts likely explain why crusts do not produce  
56 significant anomalies in other paleoclimatic records.

## 57 **1: Introduction**

58 Visual and thin-section examination of the WAIS Divide deep ice core from West  
59 Antarctica revealed an annual signal linked to bubble and grain characteristics [Fitzpatrick et al.,  
60 2014], but also numerous crusts. These crusts are bubble-free or nearly so, typically one grain and  
61 1 mm or less in thickness, and are readily identified visually in bubbly ice (Fig. 1). Their presence  
62 in greater abundance than seen in most cores [e.g., Alley, 1988] motivated studies to understand  
63 their formation, possible influence on other paleoclimatic data, and potential for recording  
64 paleoclimatic conditions themselves.

65 Work by Orsi et al. [2015] and Mitchell et al. [2015] showed that no significant artifacts  
66 are introduced to paleoclimatic records by the WAIS Divide crusts. Here, we report additional  
67 studies showing that summertime crusts form under specific conditions linked to persistent high-  
68 pressure systems, so the time-series of crusts likely contains paleoclimatic information; however,  
69 many additional issues must be addressed before useful climate histories could be constructed  
70 confidently.

71 Bubble-free layers much thicker than the bubble-free crusts discussed here are sometimes  
72 observed in ice cores from warm sites, and provide evidence of refrozen meltwater [e.g., Das and  
73 Alley, 2005]. These are of interest as paleoclimatic records but have the potential to anomalously  
74 distort records of trapped gases or other components of ice cores. Refrozen meltwater can be  
75 identified by an excess of trapped heavy noble gases, so Orsi et al. [2015] analyzed WAIS Divide  
76 samples containing bubble-free crusts, finding that not enough meltwater was involved to  
77 significantly perturb records of other trace gases. Additionally, crusts might greatly modify gas



78 trapping in the firn, but measured nitrogen-isotopic ratios at WAIS Divide show that gravitational  
79 fractionation occurs down to the normal trapping depth where normal amounts of air are trapped,  
80 demonstrating that the crusts are not both impermeable and laterally extensive at shallow depth  
81 [Mitchell et al., 2015; Battle et al., 2011].

82 Here, we report coordinated observations of crust formation over five summers (2008-09  
83 to 2012-13) at the WAIS Divide site, involving daily observations of surface evolution, shallow  
84 snow-pit studies with a 2-m pit at least once per year, insolation measurements, and near-surface  
85 temperature profiling, supplemented with data from an on-site automated weather station (AWS).

86 We find that crusts form most commonly in the summer (45% greater occurrence), but do also  
87 form in winter. In summer, crust formation primarily results from the effects of strong diurnal  
88 temperature cycling under clear-sky, low-wind, relatively warm conditions. Wintertime  
89 observations are not available, but the physical understanding gained from our summertime data  
90 suggests hypotheses for formation. Time-trends in the occurrence of summertime crusts in the  
91 core may reveal changes in the frequency of the persistent high-pressure conditions that generate  
92 crusts, although additional work will be required to quantify this.

## 93 **2: Methods**

94 The main methods used are described here. Additional details are provided in Fegyveresi  
95 [2015]. The surface was observed continually by one of us (JF) during the five field seasons  
96 extending from 2008-09 to 2012-13 (Table 1). During each austral summer, a back-lit snow pit  
97 was also prepared and studied (five total pits). All pits were sited within 1 km radius of the  
98 primary ice-core drilling facility, but avoided regions disturbed by camp operations or the “drift  
99 tail” of enhanced accumulation downwind of the camp. Following prior practice [e.g., Benson,  
100 1962; Koerner, 1971; Alley, 1988], each sampling site involved excavating a pair of ~2 m cubic

101 pits separated by a wall ~0.5 m thick, with one pit left open to supply back-light, and the other a  
102 roofed observation pit. Features such as crusts and hoar layers were easily identifiable from the  
103 observation pit on the back-lit wall (Fig. 2). Pit walls were observed, mapped, sampled, and  
104 photographed (tripod-mounted > ¼ s exposures). Each pit was oriented so the prevailing wind  
105 direction, approximately north-south, ran from right-to-left along the back-lit wall.

106 An automatic weather station (AWS) on site at WAIS Divide (named Kominko-Slade in  
107 the University of Wisconsin AWS system; Lazzara et al. [2012]), collected data on temperature,  
108 air pressure, wind, and humidity starting in the 2009-10 season (all dates and times are GMT).  
109 Beginning in 2011-12, upward-facing and downward-facing short-wave Li-Cor LI200  
110 pyranometers were added initially 1 m above the surface to measure incoming and outgoing  
111 shortwave radiation (0.4-1.1 µm spectral response). Both sensors were newly calibrated and  
112 mounted in a cosine-corrected head (for solar angles up to 80°), with typical operational errors in  
113 daylight of ±3% (max ±5%). A Kipp-Zonen CNR2 net radiometer with upward- and downward-  
114 facing pyranometers and pyrgeometers was added on an AWS mounting arm during the 2012-13  
115 season, in order to measure both net short- and long-wave radiation. [This instrumentation](#)  
116 [replaced the previous Li-Cor instrumentation.](#) The pyranometers operated with a spectral  
117 response of 0.3 – 2.8 µm, operational errors of ±3.5 %, and sensitivity of 15.21 µV W<sup>-1</sup> m<sup>-2</sup>, while  
118 the pyrgeometers operated with a spectral response of 4.5–45 µm, operational errors of ±5.6 %,  
119 and a sensitivity of 12.52 µV W<sup>-1</sup> m<sup>-2</sup> respectively; typical impedances were ~7 ohms. All AWS  
120 relative humidity values reported here are expressed in terms of saturation vapor pressure over ice  
121 [and corrected for low-temperature offsets \(see Anderson, 1994\).](#)

122 Also during the 2012-13 season, we calibrated and installed five PRD (platinum  
123 resistance detector) strings in the upper 5 m of firn in a 2 km survey line extending approximately  
124 upwind (grid-west, true-north) starting ~50 meters from the on-site AWS. The strings were

125 designed by one of us (AM) following the procedures in Muto et al. [2011]. Each sensor string  
126 was 5 m long and consisted of 16 individual PRDs (HEL-700 series;  $\pm 0.03^\circ\text{C}$  accuracy,  $\pm 0.18^\circ\text{C}$   
127 total combined error, including data-logger error) with denser sampling in the shallower firm to  
128 capture the greater variability there ([see also Supplemental Table S2](#)). Sensor calibration took  
129 place over a 60-minute period using a constantly-stirred ice-bath method, and then the newly  
130 calibrated sensors were deployed incrementally over a 10-day period starting Dec. 15<sup>th</sup>.  
131 Deployment boreholes were drilled using a 4 cm diameter hand-auger, and then back-filled once  
132 strings were installed. Campbell logging equipment (CR1000 data logger and AM/16/32  
133 Multiplexer) and 12V sealed lead-acid batteries were housed in a foam-insulated wooden box  
134 beside each borehole and just below the surface. The first string was placed 50 m from the AWS,  
135 and the other strings were placed upwind of it by 10, 100, 1000, and 2000 m (Supplemental Table  
136 [S3](#)). Measurements were taken every minute over the survey interval. Each 12V battery was  
137 swapped out weekly with newly charged replacements to ensure that the sensor strings were  
138 continually recording. During each site visit, we took photographs, and noted local  
139 meteorological and surface conditions. Each sensor string took approximately 24 hours to  
140 equilibrate with the surrounding snow following installation due to the backfilling of the open  
141 boreholes with surface snow.

142 We studied crusts in the ice core as well as in the near-surface. As described in  
143 Fitzpatrick et al. [2014], the entire deep core and various associated shallower cores were  
144 inspected visually during core processing lines at the US National Ice Core Laboratory, primarily  
145 by one of us (MS), but with some intercomparisons from other observers. The core was observed  
146 on a light table in a darkened booth, and key features were noted on meter-length log books. The  
147 crusts were easily visible as thin, glassy, bubble-free or nearly bubble-free layers (e.g. Fig. 1).

148 Annual cycles are visible in the bubbly part of the core, arising from the tendency for  
149 near-surface processes to generate coarse-grained, low-density layers including depth hoar in

150 summer [Fitzpatrick et al., 2014; Fegyveresi, 2015]. However, annual-layer dating of the ice core  
151 using electrical conductivity (ECM, which is primarily controlled by ice chemistry) and soluble-  
152 ion chemistry proved more accurate than dating with visible strata [Buizert et al., 2015; Sigl et al.,  
153 2016; WAIS Divide Project Members, 2013]. Here, we estimate the season in which each crust  
154 occurs by assigning each summertime peak in the WD2014 time scale to January 1 of its year, and  
155 then linearly interpolating; accumulation at the site is relatively evenly distributed through the  
156 year, justifying this approximation [Banta et al., 2008; Fegyveresi, 2015, Fegyveresi et al., 2016].  
157

### 158 **3: Observations**

#### 159 **3-1: Near-surface observations**

160 We summarize key observations on crust formation here. Additional information, and  
161 complete narrative descriptions of particular crust-forming episodes, are provided in Fegyveresi  
162 [2015].

163 Glazed crusts were repeatedly observed to form on the snow surface (Figs. 3 and 4),  
164 primarily during late-December and January, with an interval between formation events of  
165 roughly one and two weeks (see Figs. 5-8). Crust formation often followed a storm or wind event,  
166 and occurred during a time of higher atmospheric pressure, light winds, clear sky, strong  
167 insolation, large diurnal temperature cycling, and low relative humidity.

168 As shown in Figure 9, the crusts were often internally complex. The upper few  
169 millimeters of firn were anomalously high-density ( $> 400 \text{ kg m}^{-3}$ ) and fine-grained, and might be  
170 termed a multi-grain crust. Within this, and especially at the top, were one or more lower-porosity  
171 single-grain crusts. To an observer, light reflected off these crusts gave the appearance of a glaze  
172 on the snow surface. (e.g. Fig. 4), [see also Orsi et al., 2015, their Fig. 5].

173 Typically, a glazed crust started as isolated sub-meter to few-meter patches on unshaded  
174 regions of the snow surface or sastrugi, which were most consistently exposed to sunlight, and

Formatted: Superscript

175 | spaced tens of meters to more than 100 m apart. The spatial size and extent of glazed crusts  
176 | varied considerably and were not measured directly, however no single observed crusts patch was  
177 | greater than 100 m in length in any dimension. Over the first days of formation, glazed crusts  
178 | expanded to form a laterally extensive interconnected surface broken by isolated sub-meter to  
179 | few-meter unglazed patches on shaded faces of sastrugi. Glazed crusts were most continuous  
180 | where the surface was smoothest. Reconnaissance surveys extending a few kilometers from camp  
181 | showed that glazed-crust formation was consistent at least that far.

182 |         Within 2-3 days of formation, glazed features developed prominent polygonal cracks  
183 | with few-meter spacing (e.g. Fig. 4). It is likely that these cracks formed by thermal contraction  
184 | during nighttime cooling, which was driven by the large diurnal temperature swings observed at  
185 | the time (see below). We excavated some cracks, which could be traced downward from the  
186 | surface typically ~20-30 cm.

187 |         A pronounced hoar began forming within 24 hours of the onset of cracking of the glazed  
188 | crust in each case observed (e.g. Fig. 3). Measured relative humidity was notably higher during  
189 | hoar formation (see Figs. 5-8) than before, and sometimes (e.g., January 7<sup>th</sup>, 2010) a fog  
190 | developed early in the time of hoar formation, providing a source of vapor to the surface hoar  
191 | from above. Surface glazing was not required for formation of such hoar layers, as one formed  
192 | quickly on December 30<sup>th</sup>, 2009 during a very warm (> -10°) fog episode with elevated measured  
193 | relative humidity, but without prior formation of surface glaze.

194 |         Hoar layers that we observed during the field seasons were subsequently either buried,  
195 | destroyed by wind, or gradually sublimated away over 2-3 additional days. We observed strong  
196 | winds remove hoar layers, with a threshold of ~7 m s<sup>-1</sup> (~13 knots). In one case, hoar removal  
197 | required somewhat lower speed when wind was directed orthogonal to the prevailing direction  
198 | and thus sastrugi orientation, similar to observations by Champollion et al. [2013] at Dome C,  
199 | East Antarctica.

200 No above-freezing temperatures were observed by the AWS, but on January 2, 2011, the  
201 temperature reached a high of  $-2.8^{\circ}\text{C}$  (see Fig. 6; Supplemental Fig. S1). While no direct surface  
202 melt was observed, some melt was noted along exposed, vertically cut wall faces near the ice-  
203 core drilling facility (Supplemental Fig. S2). A prominent multi-grain crust was observed the next  
204 year in snow pits, likely dates from that time, and shows features that are consistent with some  
205 melting-refreezing having occurred (Supplemental Fig. S3).

206 The PRD strings document strong variations in subsurface temperature, following the air  
207 temperatures as expected. During the cooling phases of diurnal cycles, air temperatures (AWS)  
208 and near-surface firn temperatures (S0) dropped well below temperatures deeper in the firn  
209 including the shallowest in-firn sensor (S1) at  $\sim 20$  cm (Figs. 10 and 11), with the surface as much  
210 as  $3^{\circ}\text{C}$  colder than firn at 40 cm (S2) depth (e.g. Supplemental Fig. S4). This would have driven  
211 upward mass flux from the firn towards the surface. Such conditions often developed when  
212 surface hoar was forming from fog, and thus likely with a downward as well as an upward vapor  
213 source to the near-surface layer.

214

### 215 3-2: Snow-pit observations

216 ~~Maps of the shallow pits are presented in Fegyveresi [2015], and an additional paper~~  
217 ~~detailing the isotopic, density, and other data is planned. Relevant here, the~~Each of the five snow  
218 pits showed a clear annual cycle in the visual stratigraphy, but with notable “noise”. Depth hoars  
219 occurred primarily in summertime layers and into autumn, but with occasional hoar layers in  
220 winter and spring layers. Crusts were also most common in summertime and into autumn, but not  
221 restricted to those times. Similar to the observations made by Alley [1988] at other sites in  
222 Antarctica, sequences of strata at WAIS Divide typically showed lateral continuity over 2 m  
223 scales, although with some variation. Many graded beds were also present, likely indicative of  
224 changes during a specific storm event or primarily before the next storm. This was later

225 confirmed on-site with accumulation stakes and measurements following specific large storm  
226 events (see also Koffman et al., 2014; Criscitiello et al., 2014).

227 The snow pits from the 2008-09, 2009-10, and 2010-11 seasons at WAIS Divide were  
228 mapped here in greatest detail, and meter-wide sub-swaths of their complete pit-wall maps are  
229 shown in Fig. 12. Complex stratigraphy and variations are clearly discernable, and illustrate the  
230 variability within 1 km of each other at WAIS Divide in contiguous years. This is likely  
231 indicative of the influence of complex processes of deposition and metamorphism, with frequent  
232 occurrences of depositional and erosional features (sastrugi, whalebacks, wind scoops, hollows,  
233 etc.). We chose annual layers in the pit maps based upon visual inspection in the field,  
234 subsequent examination of photographs of the pits, and overall trends in measured densities (see  
235 e.g. Fig. 13).

236 We measured pit bulk densities using 100 cm<sup>3</sup> stainless-steel, box-type cutters [e.g.,  
237 Conger and McClung, 2009] and a digital scale accurate to 1 gram. Density samples were taken  
238 in all five concurrent seasons' pits in duplicate, at ~5 cm intervals, from the pit side-wall (so as  
239 not to disturb the back-lit wall). These duplicates were then averaged together for final values.  
240 Samples measured in the 2008-09 pit were taken with regards to marked strata, and therefore at a  
241 slightly higher frequency. Density measurements from pits of all five seasons yielded an average  
242 density of  $386.6 \pm 3.2 \text{ kg m}^{-3}$  for the upper 2 meters of firn (Fig. 14), all with a nearly identical  
243 linear trend-line slope of  $\sim 0.4 \text{ kg m}^{-3} \text{ cm}^{-1}$  with depth.

244 Seasonal interpretations of all five pits indicated an average of  $\sim 3.75$  years of  
245 accumulation recorded over the 2 meter depths, which yields an average of  $\sim 0.53 \text{ m a}^{-1}$  of  
246 accumulation at the average pit snow-density. Converted to water-equivalent, this becomes  $\sim 0.20$   
247  $\text{m a}^{-1}_{\text{w.e}}$  (or  $\sim 0.22 \text{ m a}^{-1}_{\text{ice}}$ ). These values agree closely with recently published values (WAIS  
248 Divide Project Members, 2013; Banta et al., 2008; Burgener et al., 2013), as well as oxygen  
249 isotope ratios ( $\delta^{18}\text{O}$ ) and passive microwave data in specific cases (discussed later).

250 We documented obvious crusts and hoar layers for each snow pit. Most commonly, crusts  
251 occurred just above depth hoars, but crusts were observed without hoar, and hoar without crust.  
252 Both single-grain-thick (~1 mm) and multi-grain (≥4 mm) crusts were observed, with the  
253 common association of single-grain crusts in and usually at the top of multi-grain crusts as noted  
254 above. All crusts had densities estimated over 400 kg m<sup>-3</sup>. Counting a multi-grain crust containing  
255 a single-grain crust as one feature, the five 2-meter snow pits revealed an average of ~18.8 ± 2.5  
256 (±1σ) total crusts, or approximately 5 crusts per year.

Formatted: Superscript

257 ~~Most commonly, crusts occurred just above depth hoars, but crusts were observed~~  
258 ~~without hoar, and hoar without crust. Both single-grain-thick (~1 mm) and multi-grain (≥4 mm)~~  
259 ~~crusts were observed, with the common association of single-grain crusts in and usually at the top~~  
260 ~~of multi-grain crusts as noted above. Counting a multi-grain crust containing a single-grain crust~~  
261 ~~as one feature, the 2-meter snow pits revealed an average of ~18.8 ± 2.5 (±1σ) total crusts, or~~  
262 ~~approximately 5 crusts per year.~~

### 263 3-3: Ice-core data

264 In the bubbly ice included in our crust logging (120-577 m depth) in the WAIS Divide  
265 core, 10,268 crusts were identified (Fig. 152). A few were discontinuous across the core, or  
266 displayed at least a few pores extending through; others appeared largely or completely  
267 continuous and impermeable at the scale of the core. Experience with independent observers  
268 showed little or no error in crust identification. We cannot rule out the possibility that bubble  
269 migration contributed to loss of some crusts in the deepest bubbly ice considered, but the crusts  
270 continued to be clear and readily identifiable, so we do not believe that the trend to fewer crusts  
271 in the deepest ice is an artifact. We cannot fully exclude the possibility that there is an



272 observational bias related to the drop in crust prevalence over the most recent ~250 years, as the  
273 crusts are more difficult to discern in the shallow firn.

274 |         The seasonal distribution of the crusts is shown in Figure 163. Crusts occur year-round,  
275 | but are ~45% more frequent in summertime accumulation than in wintertime. Certainly, the  
276 | natural variability in seasonal distribution of snow accumulation and in the timing of peak  
277 | impurity input mean that details of the shape of the seasonal distribution of crust occurrence are  
278 | notably uncertain. However, given the high reliability of the annual-layer dating, and the multiple  
279 | indicators that agree well [Buizert et al., 2015; Sigl et al., 2016; WAIS Divide Project Members,  
280 | 2013], “summer” versus “winter” or “nonsummer” ~~should be quite~~ are accurate well-constrained.

281 |         Time-trends of seasonal crust occurrence are also shown in Supplemental Figure S5,  
282 | separating the largely sunless winter (May-August) from the sunny spring-summer-fall  
283 | (September-April, with at least 8 hours of sunlight per day). Both first increase and then decrease  
284 | slightly over the 2400-year record, but with a larger relative change in the sunlight season.

285

286

#### 287 | **4: Synopsis and Discussion**

288 |         Our observations confirm and extend prior work on this topic. Depositional processes and  
289 | ~~diagenesis-metamorphism~~ primarily in the snow that comprises the upper few centimeters of the  
290 | firn, produce prominent layering. Wintertime accumulation, while notably variable, is more  
291 | homogeneous than summertime deposits, with wind-packed layers prominent in winter, and  
292 | more-variable layers including crusts and hoar more common in summer [e.g., Sorge, 1935;  
293 | Benson, 1962, Gow, 1965; 1969; Weller, 1969; Colbeck, 1982; Colbeck, 1983; Alley, 1988;  
294 | Alley et al., 1997]. These features are altered during subsequent burial and conversion to bubbly  
295 | ice, but still produce recognizable features in the ice core that allow identification of annual layers  
296 | and crusts [e.g., Alley et al., 1997; Fitzpatrick et al., 2014].

297 Our observations at WAIS Divide show repeating events that generate the main features  
298 of the summertime accumulation. In a typical event, a storm with strong winds brings snow  
299 accumulation, followed by a high-pressure system bringing clear skies, greatly reduced winds,  
300 initially low humidity, and strong diurnal variations in sunshine, air temperature, and net surface  
301 energy-balance.

302 Early in this clear-sky interval, the wind-packed upper surface develops a millimeter-  
303 thick glazed crust or possibly crusts in a few-millimeters-thick multi-grain crust. Strengthening of  
304 crusts over one to a few days is followed by polygonal cracking from contraction caused by  
305 nighttime cooling. Vapor released through the cracks contributes to rising relative humidity, and  
306 surface-hoar deposition in subsequent nights. At WAIS Divide, evolution of the crust-hoar  
307 complex typically is truncated by arrival of another storm, which may remove or bury the hoar,  
308 and typically buries the crusts below the level of fastest ~~diagenesis~~metamorphism, allowing them  
309 to be preserved.

310 Not every aspect of a typical event is observed in each case. Crusts form and can be  
311 buried by additional snowfall without growth of a surface hoar on top of them. Crusts are  
312 somewhat discontinuous, and surface hoar can grow where a crust is absent. And, perhaps most  
313 importantly here, a crust that remains near the surface (in the upper few centimeters) for too long  
314 may slowly lose mass and cease to be a crust.

315 Our data provide strong constraints on models of many of the observed processes.  
316 Surface hoar grew especially at night when relative humidity was high, sometimes with fog, and  
317 with deposition occurring on tent ropes or other surfaces as well as on the snow surface (e.g.  
318 Supplemental Fig. S6), clearly demonstrating a source of vapor from above. Surface hoar  
319 typically formed however, when the upper snow surface was colder than layers beneath,  
320 indicating a vapor source from below ~~as well~~. Hence, our surface hoars included elements of both

321 depositional and sublimation hoar crystals as defined by Gallet et al. [2014] based on  
322 observations at Dome C, East Antarctica [\(with sublimation growth being the dominant process\)](#).-

323         The high density of both single-grain and multi-grain crusts, approaching the density of  
324 ice for the glassy single-grained crusts, requires that the density of the crusts was increased over  
325 time, as wind packing has not been observed to approach these high densities. Crusts form during  
326 days when atmospheric humidity is low, however, and thus when mass is not being added from  
327 above. We have not observed bulk melting at the site (with the one possible exception noted  
328 above), nor do the gas measurements of Orsi et al. [2015] indicate bulk melting, so the density  
329 increase must arise from some combination of vapor diffusion from below and surface or volume  
330 mass transfer likely involving pseudo-liquid layers [Dash et al., 2006], as discussed next.

331         The data here show that frequently the upper surface is colder than snow beneath, which  
332 will lead to upward mass flux. We lack subcentimetric resolution in thermometry, but physical  
333 understanding indicates that very strong gradients likely develop on the centimeter scale just  
334 below the upper surface during rapid nighttime cooling. Physical understanding, the data here,  
335 and data from previously published studies indicate that intense sunshine generates a temperature  
336 maximum in the snow just below the surface (order of 1 cm) especially in low-density, low-  
337 thermal-conductivity depth hoar [e.g., Alley et al., 1990; Brandt and Warren, 1993], also  
338 contributing to upward vapor transport. Hence, the upper surface is expected to gain mass from  
339 below during the crust- and hoar-forming events [Alley et al., 1990]. Windy conditions would  
340 drive undersaturated air into and out of pore spaces, removing mass, but crusts form during  
341 relatively still times. The temperature gradients [\(and noted inversions\)](#) measured here at WAIS  
342 Divide [\(see also Figures 10 and 11, and Supplemental Figure S4\)](#) are similar to those observed at  
343 GISP2 by Alley et al. [1990] and more than sufficient to move the necessary vapor for crust  
344 development.

345           We hypothesize here that these surface conditions cause mass fluxes that fill in open  
346 pores in wind-packed layers at the surface to form glazed crusts. A physical model might be  
347 based on the following considerations. The thermal conductivity of ice greatly exceeds that of air,  
348 so heat transport in firm is primarily conductive. Ordinarily, the grain curvature adjacent to pores  
349 tends to cause diffusive mass loss, enlarging pores by filling necks between grains or other  
350 regions of lower vapor pressure. However, because heat flow is primarily through the grain  
351 structure, pores in a surface crust will tend to be colder than interconnected grains when the upper  
352 surface is colder than the firm beneath, favoring mass transport to the pore surfaces, as shown in  
353 Figure 174 [e.g., Sommerfeld, 1983; Fukuzawa and Akitaya, 1993]. Transport may occur by  
354 vapor, surface, or volume diffusion; following Alley and Fitzpatrick [1999], vapor diffusion and  
355 surface transport in premelted films are likely to dominate. Also, mass loss from relatively warm  
356 grain bonds just beneath a growing surface crust by diffusion to the colder crust will tend to lower  
357 the crust, increasing the likelihood that a pore in the crust will move downward to intersect a pre-  
358 existing grain beneath, increasing the crust density.

359           Although summertime crusts dominate in the ice core, many wintertime crusts were  
360 identified, raising additional questions. We lack direct observations in winter, and so can only  
361 speculate on mechanisms active then. However, the basic picture drawn above for summertime  
362 crusts may also apply in winter. The lower temperatures, and lack of intense solar heating, make  
363 crust formation less likely. However, stronger wintertime winds would allow greater wind-  
364 packing of the upper surface, producing fewer and smaller pores to be filled to make a thin crust,  
365 and thus making crust formation easier. Although accumulation is more-or-less evenly distributed  
366 through the year, we speculate (based upon variability observed in AWS data) that there may be  
367 extended intervals up to weeks in length during the winter when the surface is relatively stable,  
368 partially or completely offsetting the slower mass transport from colder temperatures.  
369 Furthermore, the AWS data show that mid-winter temperatures have risen as high as  $-15^{\circ}\text{C}$

370 during strong warming events accompanied by high winds ( $> 10 \text{ m s}^{-1}$ ), and likely linked to  
371 transport of air masses from the coast. Such warm ~~and windy~~ air masses paired with these high  
372 winds, would produce relatively high vapor pressures, contribute to greater surface packing, and  
373 promote temperature inversions and upward near-surface vapor flux during the subsequent  
374 cooling.

375 The great abundance of crusts at WAIS Divide compared to other ice cores we have  
376 studied may be because conditions are “just right” at WAIS Divide. We have observed loss of a  
377 wind-packed crust at WAIS Divide, and also at GISP2 in central Greenland; the strong mass loss  
378 from ~1 cm down in the snowpack is not conducive to long-term survival of any crust there [e.g.,  
379 Alley et al., 1990]. Low but nonzero summertime accumulation thus may lead to loss of crusts,  
380 whereas higher accumulation after formation buries them below that zone of mass loss and so  
381 allows their preservation. The large wintertime variability and high wintertime temperatures at  
382 WAIS Divide may be important in generating sufficiently high mass fluxes to produce wintertime  
383 crusts.

384 At least in summertime, crusts do seem to record a particular meteorological pattern of  
385 storms alternating with still conditions. The time-series of frequency of occurrence of crusts thus  
386 would be affected by a change in the frequency of occurrence of these conditions. Turning this  
387 into a paleoclimatic indicator would require additional steps, however, as the frequency of  
388 preserved crusts could decrease because fewer were formed or because more were destroyed,  
389 with different causes. Information on changing frequency of meteorological events might be  
390 useful [e.g., Hammer, 1985; Alley, 1988]. We believe that the clear association of crust formation  
391 with particular events, and the clear trends in crust occurrence in the core, motivate additional  
392 research on topics including crust formation in non-summer seasons, but we do not know whether  
393 this ultimately could yield a valuable paleoclimatic indicator.

394 **5: Conclusions**

395           Summertime observations at the WAIS Divide site show that prominent visible strata  
396 form at or very near the surface during summer, by processes that typically are repeated a few  
397 times during each summer. A storm produces a wind-packed layer. The following high-pressure  
398 system brings light winds, warm days and cool nights, strong sunshine, and low relative  
399 humidity. High-density, single-grain-thick glazed crusts preferentially form at the surface during  
400 these high-pressure intervals, in as little as a single day, and then strengthen and evolve. Crusts  
401 are extensive, although typically broken by sub-meter or few-meter uncrusted regions spaced tens  
402 of meters to more than 100 m apart. Daytime solar heating drives upward mass transport to crusts  
403 from developing depth hoar beneath, strengthening the crusts. After formation, crusts are broken  
404 by polygonal cracks extending typically 20-30 cm deep, likely from contraction during nighttime  
405 cooling. Relative humidity then rises in the air above, contributing to growth of surface hoar  
406 during nighttime cooling. Subsequent storms typically bury the crust-hoar complexes, although  
407 crusts can be lost during evolving surface conditions if not buried below the top one to a few  
408 centimeters.

409           Study of the WAIS Divide deep core shows that crusts are preserved through the bubbly  
410 ice. Crusts are most common in layers deposited during summertime, but also occur in winter  
411 accumulation. Study of AWS data suggests that the intrusion of warm coastal air during winter  
412 may generate strong temperature gradients, which may contribute to wintertime crust formation  
413 in wind-packed layers.

414           The frequency of occurrence of crusts in the core varies with time, suggesting the  
415 possibility that crusts could be used as a paleoclimatic indicator. However, additional work  
416 would be required, including addressing whether crust frequency varies because of changes in  
417 formation or changes in destruction of crusts previously formed. The crusts do not produce

418 significant anomalies in other ice-core paleoclimatic records, likely at least in part because they  
419 are discontinuous and broken by contraction cracks.

420 **6: Data Availability:**

421 Data policy: All data presented here are available via download from NSIDC  
422 (<http://nsidc.org>) or from the WAIS Divide data portal (<http://waisdivide.unh.edu>).  
423

424 **7: Author Contribution:**

425 A.J. Orsi assisted with field observations and experiments. A. Muto designed the near-  
426 surface PRD sensor strings and developed the associated logging code. M. Spencer documented  
427 all ice-core crust observations during the WAIS Divide core processing at the National Ice Core  
428 Laboratory. J.M. Fegyveresi and R.B. Alley prepared the manuscript with contributions from all  
429 co-authors.  
430

431 **8: Acknowledgements:**

432           We acknowledge the following funding sources for support of this work: U.S. National  
433 Science Foundation Division of Polar Programs grants 0539578, 1043528, 1142085, 1619793.  
434 We also acknowledge Donald E. Voigt, Joan J. Fitzpatrick, Eric D. Cravens, and the staff of the  
435 U.S. National Ice Core Laboratory in Denver, Colorado, as well as the WAIS Divide Science  
436 Coordination Office at the University of New Hampshire, and the Ice Drilling Design and  
437 Operations group at the University of Wisconsin. We thank numerous colleagues involved with  
438 the WAIS Divide project, especially Kendrick Taylor, Mark Twickler, and Joseph Souney. We  
439 thank Bess Koffman, Gifford Wong, Dominic Winski, Aron Buffen, and Logan Mitchell for  
440 assistance with snow pit preparation. Lastly we thank Jonathan Thom and the University of  
441 Wisconsin-Madison Automatic Weather Station Program for assistance with weather station  
442 sensor installation. Any use of trade, firm, or product names is for descriptive purposes only and  
443 does not imply endorsement.

444

445



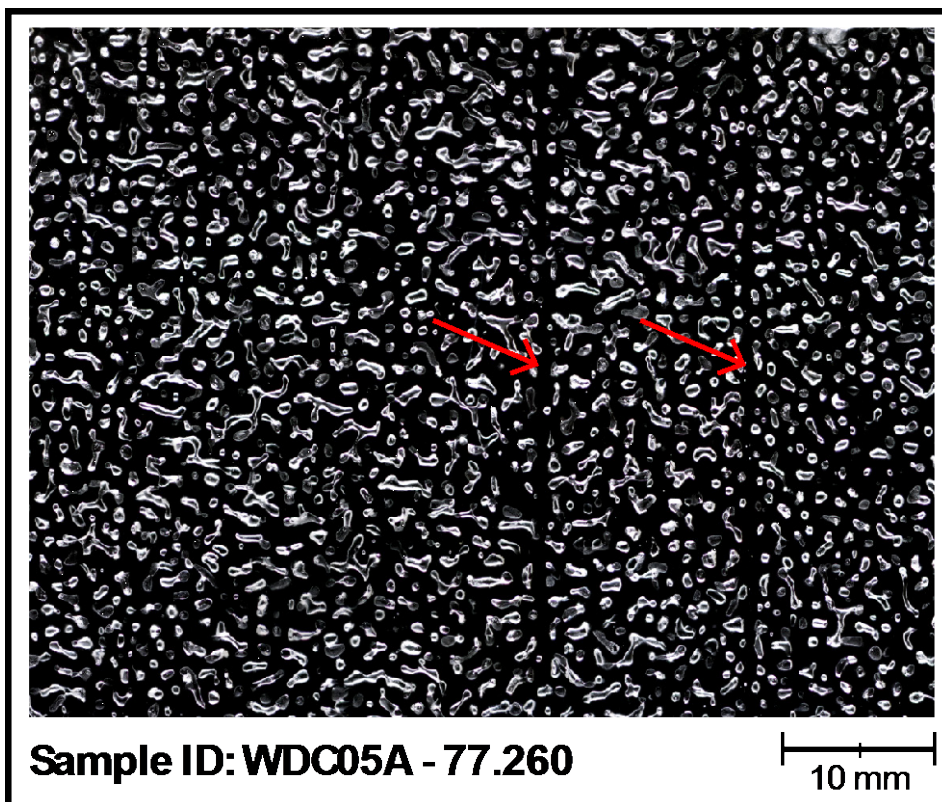
446 **9: References**

- 447 Alley, R.B., 1988. Concerning the deposition and diagenesis of strata in polar firn. *Journal of*  
448 *Glaciology*, 34: 283-290.
- 449 Alley, R.B., Saltzman, E.S., Cuffey, K.M. and Fitzpatrick, J.J., 1990. Summertime formation of  
450 depth hoar in central Greenland. *Geophysical Research Letters*, 17(13): 2393-2396,  
451 doi:[10.1029/GL017i013p02393](https://doi.org/10.1029/GL017i013p02393).
- 452 Alley, R.B. and Fitzpatrick, J.J., 1999. Conditions for bubble elongation in cold ice-sheet ice.  
453 *Journal of Glaciology*, 45(149): 147-153.
- 454 Alley, R.B., Shuman, C.A., Meese, D.A., Gow, A.J., Taylor, K.C., Cuffey, K.M., Fitzpatrick, J.J.,  
455 Grootes, P.M., Zielinski, G.A., Ram, M. and Spinelli, G., 1997. Visual- stratigraphic  
456 dating of the GISP2 ice core: Basis, reproducibility, and application. *Journal of*  
457 *Geophysical Research: Oceans*, 102(C12): 26367-26381, doi:[10.1029/96JC03837](https://doi.org/10.1029/96JC03837).
- 458 [Anderson, P.S., 1994. A method for rescaling humidity sensors at temperatures well below](#)  
459 [freezing. \*Journal of Atmospheric and Oceanic Technology\*, 11\(5\), 1388-1391.](#)
- 460 [Anderson, D. L., and Benson C.S., 1963. The densification and diagenesis of snow. in \*Ice and\*](#)  
461 [Snow: Properties, Processes and Applications](#), edited by W. D. Kingery, pp. 391–411,  
462 [MIT Press.](#)
- 463 Banta, J.R., McConnell, J.R., Frey, M.M., Bales, R.C. and Taylor, K., 2008. Spatial and temporal  
464 variability in snow accumulation at the West Antarctic Ice Sheet Divide over recent  
465 centuries. *Journal of Geophysical Research: Atmospheres*, 113(D23), doi:  
466 [10.1029/2008JD010235](https://doi.org/10.1029/2008JD010235).
- 467 Battle, M.O., Severinghaus, J.P., Sofen, E.D., Plotkin, D., Orsi, A.J., Aydin, M., Montzka, S.A.,  
468 Sowers, T. and Tans, P.P., 2011. Controls on the movement and composition of firn air at  
469 the West Antarctic Ice Sheet Divide. *Atmospheric Chemistry and Physics*, 11(21), 11007-  
470 11021, doi:[10.5194/acp-11-11007-2011](https://doi.org/10.5194/acp-11-11007-2011).
- 471 Benson, C.S., 1962. Stratigraphic Studies on Greenland Ice Sheet and a Quantitative  
472 Classification of Glaciers. *Bulletin of the American Meteorological Society*, 43(4): 141.
- 473 Brandt, R.E. and Warren, S.G., 1993. Solar-heating rates and temperature profiles in Antarctic  
474 snow and ice. *Journal of Glaciology*, 39(131), 99-110.
- 475 Buizert, C. et al., 2015. The WAIS Divide deep ice core WD2014 chronology—Part 1: Methane  
476 synchronization (68–31 ka BP) and the gas age–ice age difference. *Climate of the Past*,  
477 11(2): 153-173, doi:[10.5194/cp-11-153-2015](https://doi.org/10.5194/cp-11-153-2015).
- 478 [Burgener, L., Rupper, S., Koenig, L., Forster, R., Christensen, W.F., Williams, J., Koutnik, M.,](#)  
479 [Miege, C., Steig, E.J., Tinge, D., Keeler, D., and Riley, L., 2013. An observed negative](#)  
480 [trend in Antarctic accumulation rates from 1975 to 2010: Evidence from new observed](#)  
481 [and simulated records. \*Journal of Geophysical Research-Atmospheres\*, 118\(10\): 4205-](#)  
482 [4216.](#)
- 483 Champollion, N., Picard, G., Arnaud, L., Lefebvre, E. and Fily, M., 2013. Hoar crystal  
484 development and disappearance at Dome C, Antarctica: observation by near-infrared  
485 photography and passive microwave satellite. *The Cryosphere*, 7(4): 1247-1262,  
486 doi:[10.5194/tc-7-1247-2013](https://doi.org/10.5194/tc-7-1247-2013).
- 487 Colbeck, S.C., 1982. An overview of seasonal snow metamorphism. *Reviews of Geophysics*,  
488 20(1): 45-61.
- 489 Colbeck, S.C., 1983. Theory of metamorphism of dry snow. *Journal of Geophysical Research:*  
490 *Oceans*, 88(C9): 5475-5482.
- 491 [Conger, S.M., McClung, D.M., 2009. Comparison of density cutters for snow profile](#)  
492 [observations. \*Journal of Glaciology\*, 55\(189\): 163-169.](#)
- 493 [Crisciello, A.S., Das, S.B., Karnauskas, K.B., Evans, M.J., Frey, K.E., Joughin, I., Steig, E.J.,](#)

494 [McConnell, J.R., and Medley, B., 2014. Tropical Pacific Influence on the Source and](#)  
495 [Transport of Marine Aerosols to West Antarctica. \*Journal of Climate\*, 27\(3\): 1343-1363.](#)  
496 Das, S.B. and Alley, R.B., 2005. Characterization and formation of melt layers in polar snow:  
497 observations and experiments from West Antarctica. *Journal of Glaciology*, 51(173):  
498 307-312, doi:[10.3189/172756505781829395](#).  
499 Dash, J.G., Rempel A.W., and Wettlaufer J.S., 2006. The physics of premelted ice and its  
500 geophysical consequences, *Rev. Mod. Phys.* 78, 695-741,  
501 doi:[10.1103/RevModPhys.78.695](#).  
502 Fegyveresi, J.M., 2015, Physical properties of the West Antarctic Ice Sheet (WAIS) Divide deep  
503 core: Development, evolution, and interpretation, PhD thesis, The Pennsylvania State  
504 Univ., State College, Pa.  
505 Fegyveresi, J.M., Alley, R.B., Fitzpatrick, J.J., Cuffey, K.M., McConnell, J.R., Voigt, D.E.,  
506 Spencer, M.K. and Stevens, N.T., 2016. Five millennia of surface temperatures and ice  
507 core bubble characteristics from the WAIS Divide deep core, West Antarctica.  
508 *Paleoceanography*, 31: 416–433, doi:[10.1002/2015PA002851](#).  
509 Fitzpatrick, J.J., Voigt, D.E., Fegyveresi, J.M., Stevens, N.T., Spencer, M.K., Cole-Dai, J., Alley,  
510 R.B., Jardine, G.E., Cravens, E.D., Wilen, L.A. and Fudge, T.J., 2014. Physical  
511 properties of the WAIS Divide ice core. *Journal of Glaciology*, 60(224), 1181-1198,  
512 doi:[10.3189/2014JoG14J100](#).  
513 Fukuzawa, T. and Akitaya E., 1993. Depth-Hoar Crystal-Growth in the Surface-Layer under  
514 High-Temperature Gradient. *Annals of Glaciology*, 18: 39-45.  
515 Gallet, J.C., Domine, F., Savarino, J., Dumont, M. and Brun, E., 2014. The growth of sublimation  
516 crystals and surface hoar on the Antarctic plateau. *The Cryosphere*, 8(4): 1205-1215,  
517 doi:[10.5194/tc-8-1205-2014](#).  
518 Gow, A. 1965. On the accumulation and seasonal stratification of snow at the South Pole. *Journal*  
519 *of Glaciology*, 5(40): 467-477.  
520 Gow, A. 1969. On the rates of growth of grains and crystals in south polar firn. *Journal of*  
521 *Glaciology*, 8(53): 241-252.  
522 Hammer, C.U., 1985. The influence on atmospheric composition of volcanic eruptions as derived  
523 from ice-core analysis. *Annals of Glaciology*, 7: 125-129.  
524 Koerner, R.M. 1971. A stratigraphic method of determining the snow accumulation at Plateau  
525 Station, Antarctica, and application to South Pole-Queen Maud Land traverse 2, 1965-  
526 1966. In Crary, A.P. *Antarctic snow and ice studies II*, (Washington, DC, American  
527 Geophysical Union): 225-238.  
528 [Koffman, B.G., Kreutz, K.J., Breton, D.J., Kane, E.J., Winski, D.A., Birkel, S.D., and Kurbatov,](#)  
529 [A.V., 2014. Centennial-scale variability of the Southern Hemisphere westerly wind belt](#)  
530 [in the eastern Pacific over the past two millennia. \*Climate of the Past\*, 10\(3\): 1125-1144.](#)  
531 Lazzara, M.A., Weidner, G.A., Keller, L.M., Thom J.E., and Cassano, J.J., 2012. Antarctic  
532 Automatic Weather Station Program 30 Years of Polar Observations. *Bulletin of the*  
533 *American Meteorological Society*, 93(10): 1519-1537, doi:[10.1175/BAMS-D-11-](#)  
534 [00015.1](#).  
535 Mitchell, L.E., Buizert, C., Brook, E.J., Breton, D.J., Fegyveresi, J., Baggenstos, D., Orsi, A.,  
536 Severinghaus, J., Alley, R.B., Albert, M. and Rhodes, R.H., 2015. Observing and  
537 modeling the influence of layering on bubble trapping in polar firn. *Journal of*  
538 *Geophysical Research: Atmospheres*, 120(6): 2558-2574, doi:[10.1002/2014JD022766](#).  
539 Muto, A., Scambos, T.A., Steffen, K., Slater, A.G. and Clow, G.D., 2011. Recent surface  
540 temperature trends in the interior of East Antarctica from borehole firn temperature  
541 measurements and geophysical inverse methods. *Geophysical Research Letters*, 38(15),  
542 doi:[10.1029/2011GL048086](#).

- 543 Orsi, A.J., Kawamura, K., Fegyveresi, J.M., Headly, M.A., Alley, R.B. and Severinghaus, J.P.,  
544 2015. Differentiating bubble-free layers from melt layers in ice cores using noble gases.  
545 *Journal of Glaciology*, 61(227): 585-594, doi:[10.3189/2015JoG14J237](https://doi.org/10.3189/2015JoG14J237).  
546 Sigl, M. et al., 2016. The WAIS Divide deep ice core WD2014 chronology–Part 2: Annual-layer  
547 counting (0–31 ka BP). *Climate of the Past*, 12(3): 769-786, doi:[10.5194/cp-12-769-](https://doi.org/10.5194/cp-12-769-2016)  
548 [2016](https://doi.org/10.5194/cp-12-769-2016).  
549 Sommerfeld, R.A., 1983. A branch grain theory of temperature gradient metamorphism in snow.  
550 *Journal of Geophysical Research: Oceans*, 88(C2): 1484-1494,  
551 doi:[10.1029/JC088iC02p01484](https://doi.org/10.1029/JC088iC02p01484).  
552 Sorge, E., 1935. Glaziologische Untersuchungen in Eismitte. *Brockamp, B., and others.*  
553 *Glaziologie. Leipzig, FA Brockhaus*, 935: 62-270.  
554 WAIS Divide Project Members, 2013. Onset of deglacial warming in West Antarctica driven by  
555 local orbital forcing. *Nature*, 500(7463): 440-444, doi:[10.1038/nature12376](https://doi.org/10.1038/nature12376).  
556 Weller, G. 1969. The heat and mass balance of snow dunes on the central Antarctic Plateau.  
557 *Journal of Glaciology*, 8: 277-284.  
558  
559 |

560



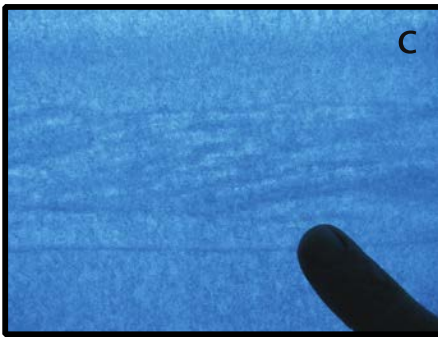
561  
562  
563  
564  
565  
566  
567  
568

**Figure 1:** A thick-section image of a sample prepared from a depth of ~77.260 meters showing two preserved crusts. Both layers are ~1 mm thick and appear mostly bubble-free. All bubbles here appear white, with the surrounding ice black. The general elongated shape of the bubbles is due the proximity of this sample to the bubble close-off depth at WAIS Divide of ~75 meters). This sample is from the secondary WDC05A core at the WAIS Divide site. Image modified from Orsi et al. [2015].



a

b

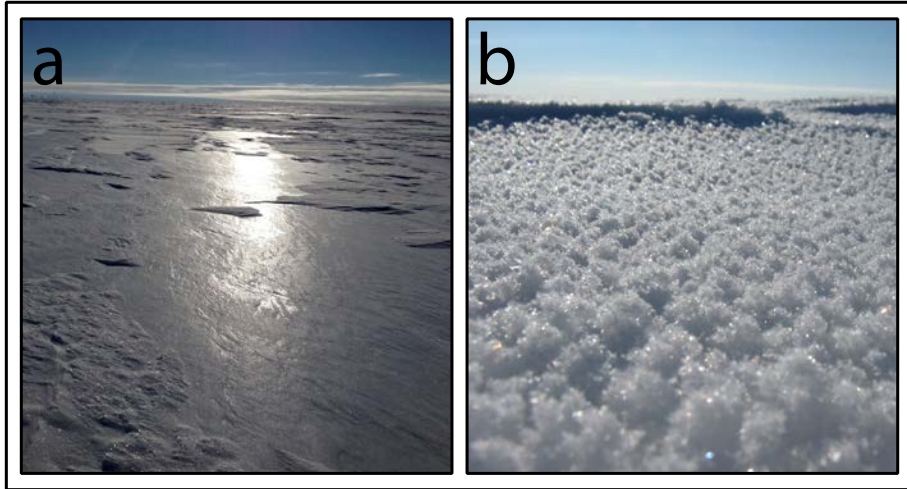


c

d

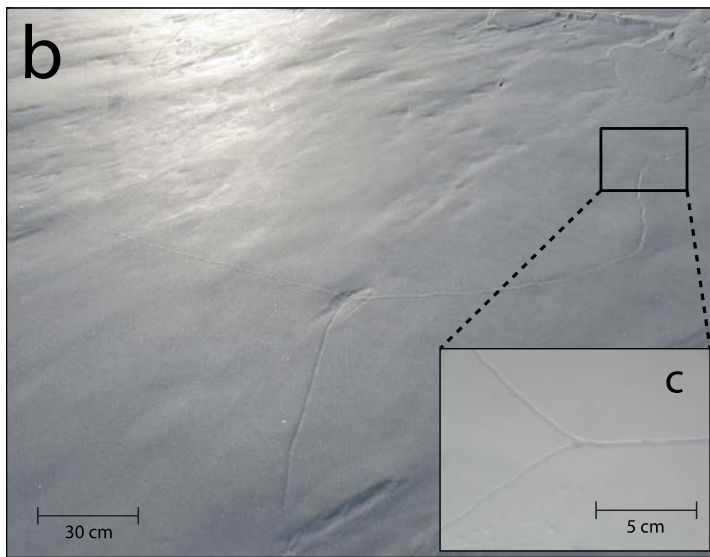
569  
570  
571  
572  
573

**Figure 2:** The lead author in a 2-meter snow pit prepared at WAIS Divide (pit 2009-10-A). Multi-grain crusts (a, b), preserved sastrugi with cross-bedding (c), and hoar layers (d) are all easily identifiable.



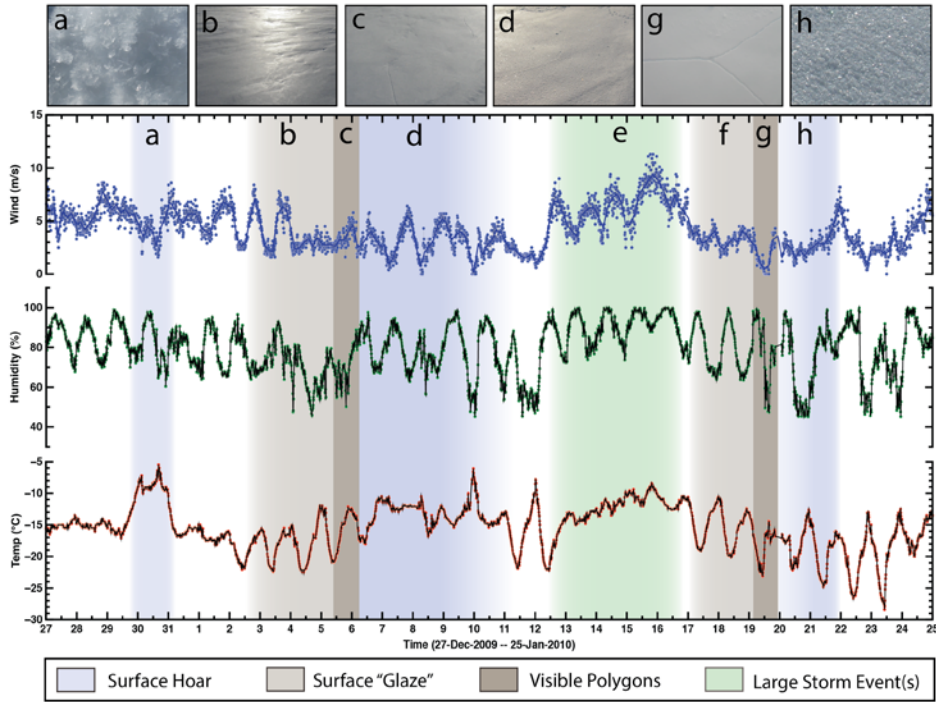
574  
575  
576

**Figure 3:** Surface “glaze” (a) that formed on a calm, sunny day (23-Dec-2012) at WAIS Divide, and the subsequent surface hoar layer (b) that formed on its surface after several calm days.



577  
578  
579  
580  
581

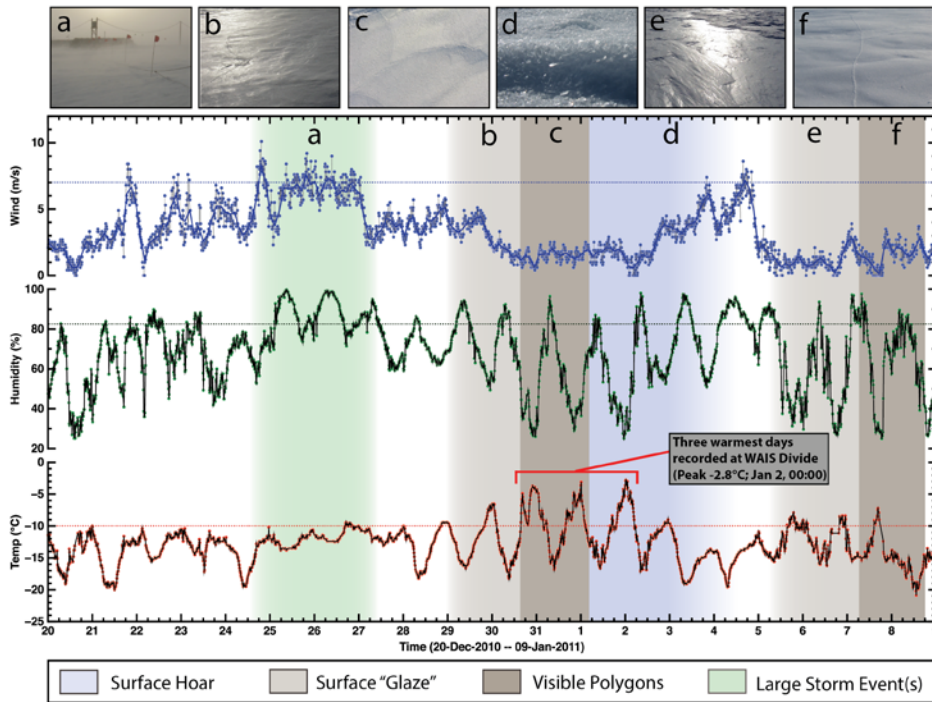
**Figure 4:** Surface “glaze” seen at the WAIS Divide site. (a). A zoomed-in view shows the polygonal cracking that initiates at the surface from thermal contraction, following several sunny, clear-sky days (b). Closer inspection reveals greater detail and scale of a crack triple-junction (c).



582  
583  
584  
585  
586  
587  
588

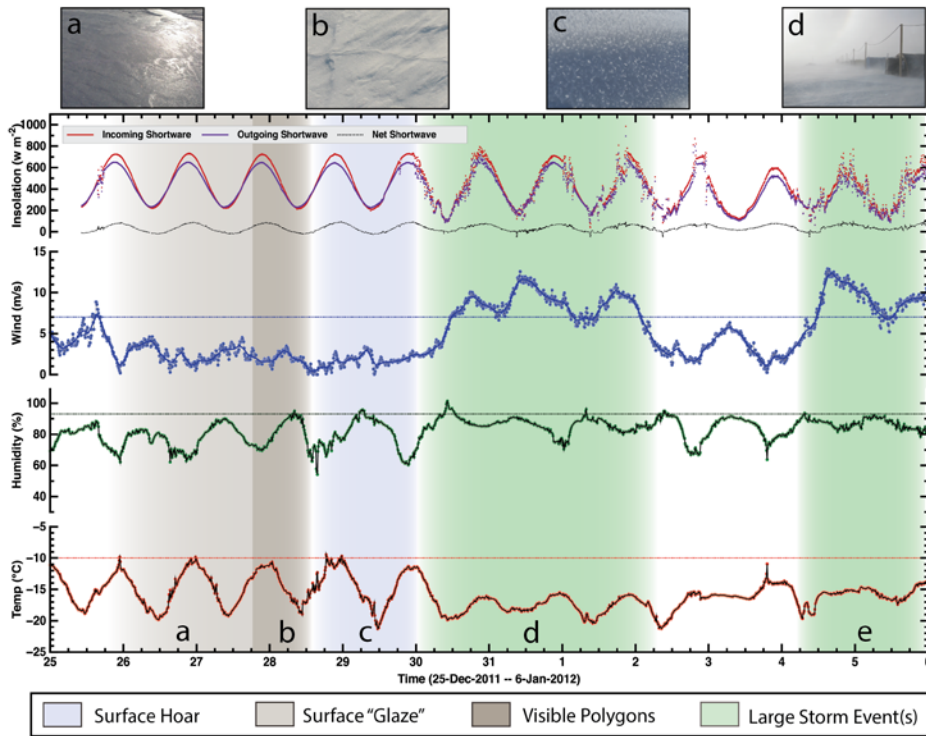
**Figure 5:** Surface evolution over 29 days in 2009-10 season, and AWS data. Shading shows episodes of surface hoar, glazes, and polygonal cracking; storm events are also shown. Letters near the top refer to photographs above of specific features or events. All dates and times are GMT (-12 WAIS local time). The errors for all AWS instruments are listed in Supplemental Table S1.





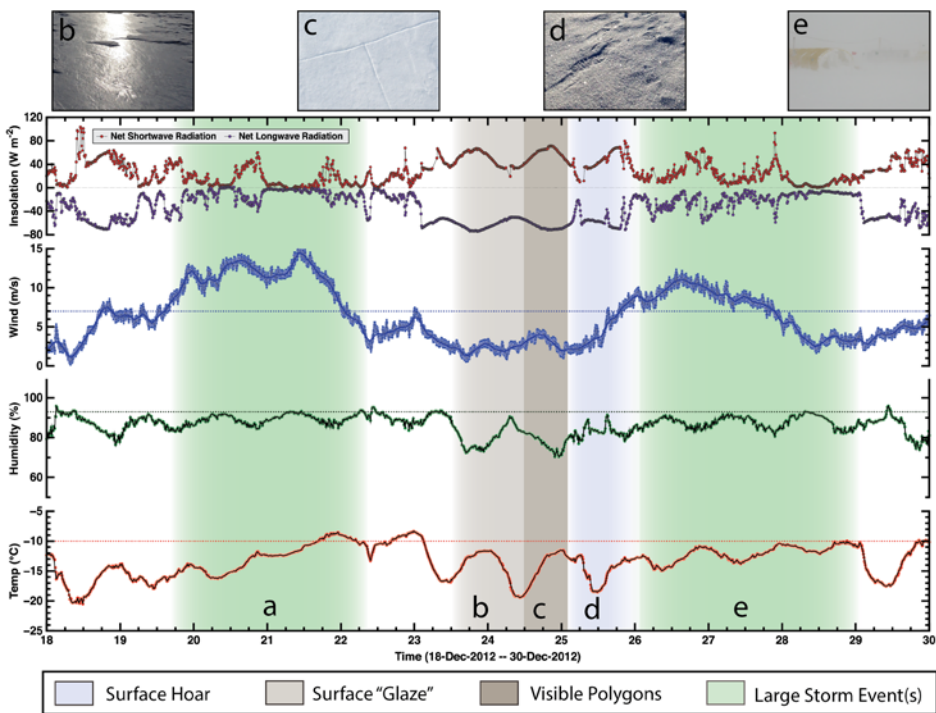
589  
 590  
 591  
 592  
 593  
 594  
 595

**Figure 6:** Surface evolution over 20 days in 2010-11 season, and AWS data. Shading shows episodes of surface hoar, glazes, and polygonal cracking; storm events are also shown. Letters near the top refer to photographs above of specific features or events. All dates and times are GMT (-12 WAIS local time). The errors for all AWS instruments are listed in Supplemental Table S1.



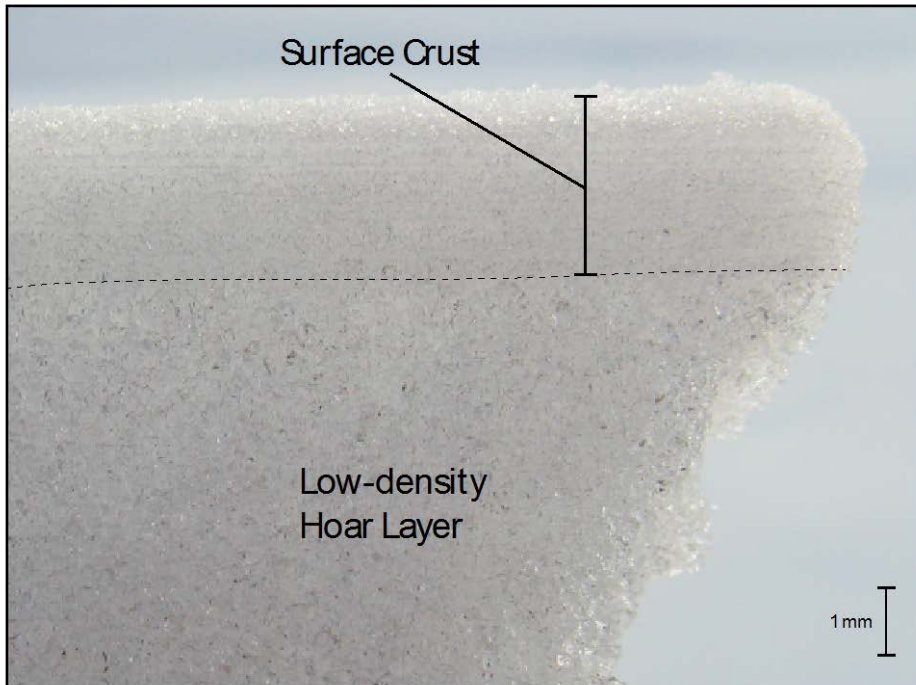
596  
 597  
 598  
 599  
 600  
 601  
 602

**Figure 7:** Surface evolution over 12 days in 2011-12 season, and AWS data. Shading shows episodes of surface hoar, glazes, and polygonal cracking; storm events are also shown. Letters near the top refer to photographs above of specific features or events. All dates and times are GMT (-12 WAIS local time). The errors for all AWS instruments are listed in Supplemental Table S1.



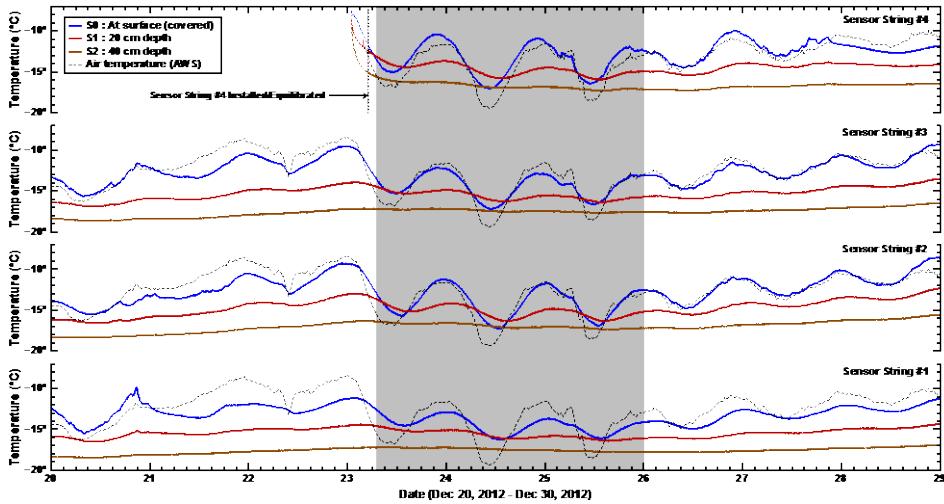
603  
604  
605  
606  
607  
608  
609

**Figure 8:** Surface evolution over 12 days in 2012-13 season, and AWS data. Shading shows episodes of surface hoar, glazes, and polygonal cracking; storm events are also shown. Letters near the top refer to photographs above of specific features or events. All dates and times are GMT (-12 WAIS local time). The errors for all AWS instruments are listed in Supplemental Table S1.



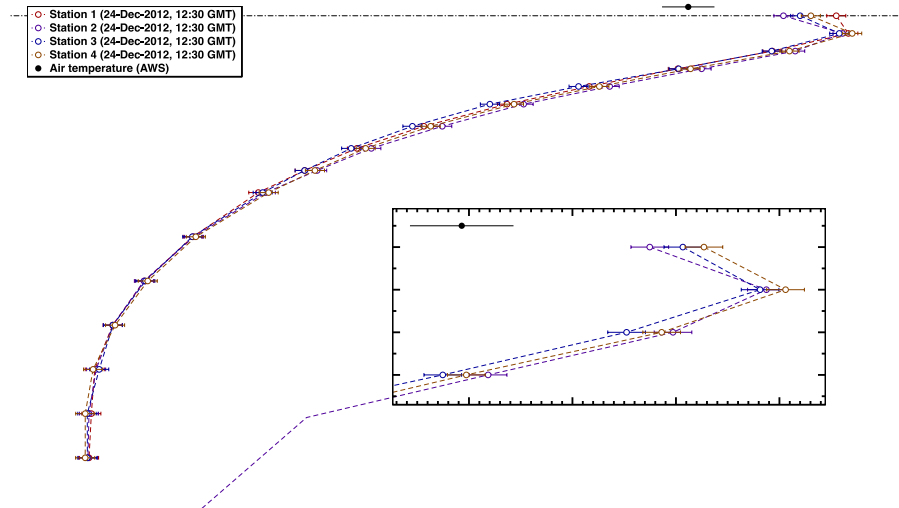
610  
611  
612  
613  
614  
615

**Figure 9:** A firm sample excavated from a glazed area at WAIS Divide before the onset of polygonal cracking, showing a couplet of an evolved high-density ( $> 400 \text{ kg m}^{-3}$ ), ~3 mm multi-grain surface crust containing single-grain crusts, and overlying a lower-density ( $< 300 \text{ kg m}^{-3}$ ) hoar layer.



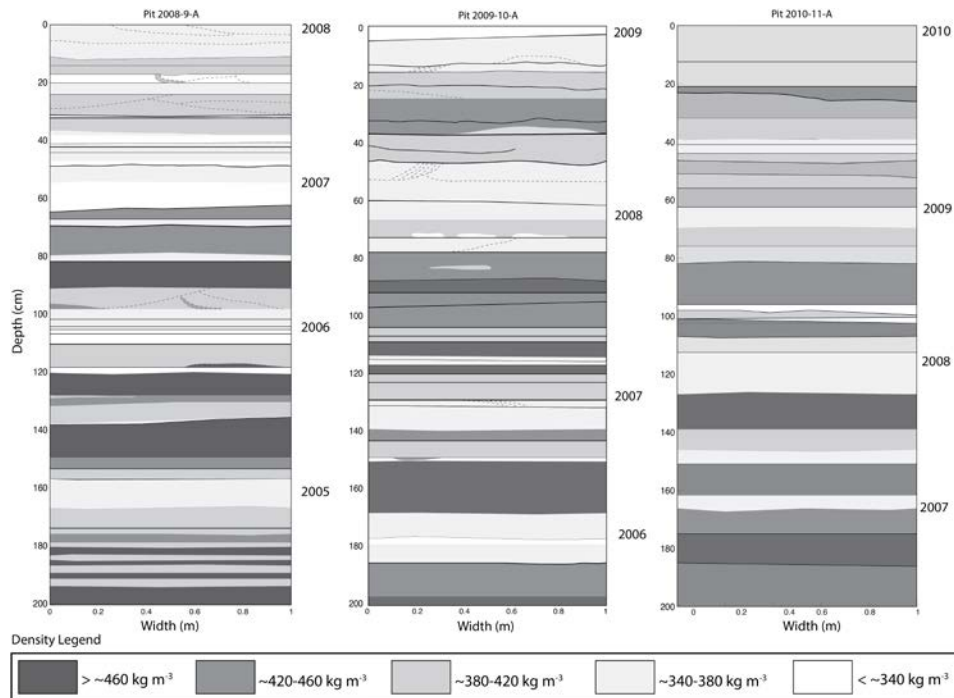
616  
 617  
 618  
 619  
 620  
 621  
 622  
 623  
 624  
 625

**Figure 10:** Temperature measurements (1 min interval) in firm from the 2012-13 season, from the upper-most three PRDs (surface down to 40 cm). Data are from the four sensor stations closest to the station. The shaded area corresponds to an episode of glaze and hoar growth (see Fig. 8). Distinct near-surface temperature inversions occurred each night during this 3-day period (see Fig. 11). Sensor #4 was not installed until Dec 22<sup>nd</sup>, and therefore did not equilibrate until early on the 23<sup>rd</sup> as indicated. Air temperature is also shown as recorded by the AWS (errors listed in Supplemental Table S1). The AWS temperature sensor is located ~1 meter above the snow surface. All dates and times are GMT (-12 WAIS local time).



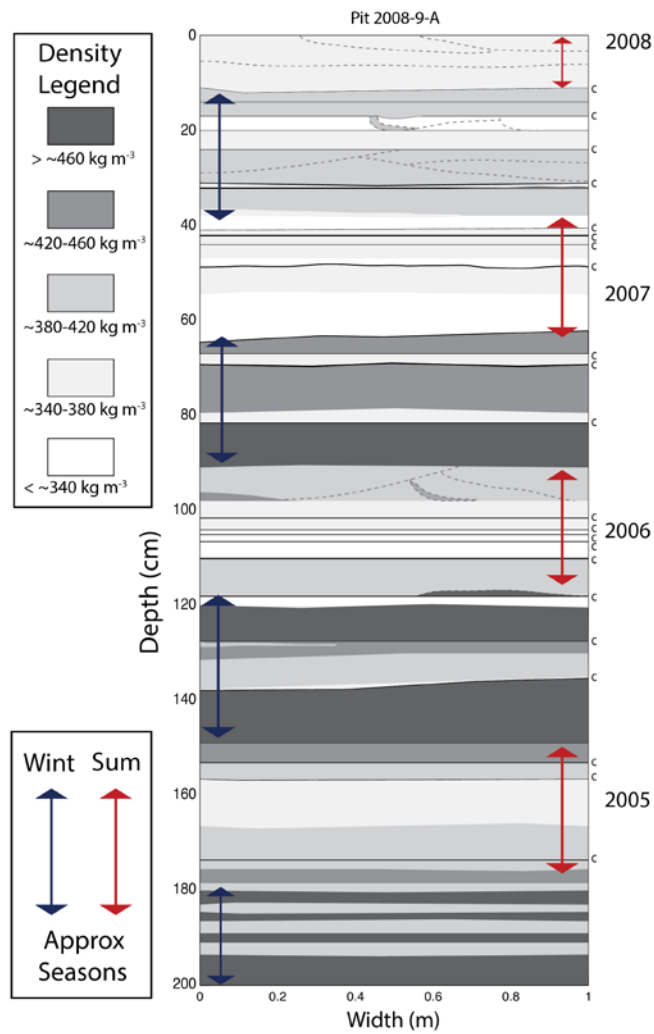
626  
 627  
 628  
 629  
 630

**Figure 11:** Snap-shot temperature readings for PRD-string stations #1-4, taken on 24-Dec-2012 at ~12:30 GMT, showing the temperature inversion with colder air (AWS data) and upper surface over warmer near-surface firm.



631  
632  
633  
634  
635  
636  
637  
638  
639  
640

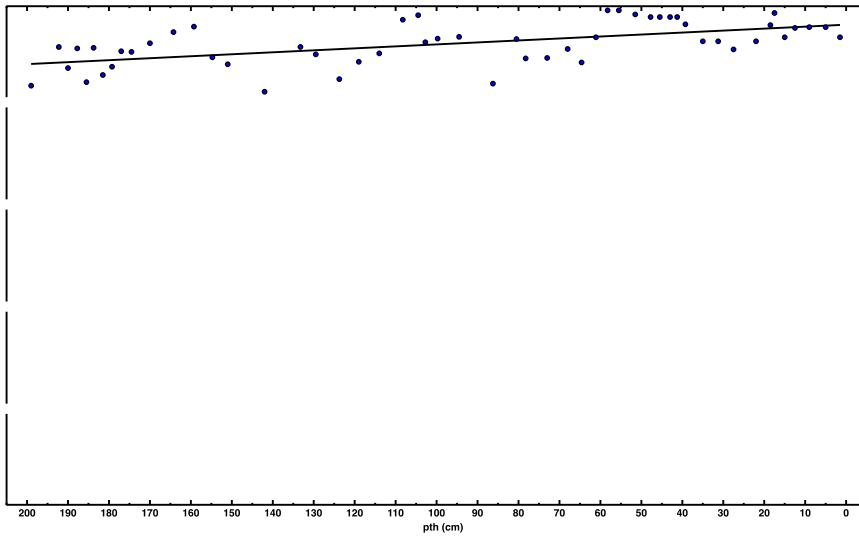
**Figure 12:** Complete wall maps of back-lit snow pits prepared during 2008-09, 2009-10, and 2010-11 WAIS Divide field seasons. Layering and density contrast are noted by degree of shading. Fine- to medium- grained, higher-density snow/firn layers are shown with darker grey coloring, whereas coarse-grained and low-density layers (e.g., depth hoar) are shown in white. Crusts are indicated with solid lines, while dotted lines are used to represent cross-bedding at depth. Years were identified based on approximate depths of peak summers and the average measured densities. The pit wall surfaces trend in parallel with the prevailing wind direction at WAIS Divide (approximately north-south, with north to the right).



641  
 642  
 643  
 644  
 645  
 646  
 647  
 648

**Figure 13:** A detailed view of data for snow pit 2008-09-A, including wall map, density profile, annual layer picks, and crusts occurrences. Density, layering, and feature preservation are again noted as in Fig. 12. Individual crusts are identified with a labeled “c” along the vertical axis. Seasonal accumulation layers “picked” visually in the pit (shown with red and blue arrows). These observations indicate a somewhat regular pattern of equally-distributed yearly accumulation at WAIS Divide with clear annual signals.

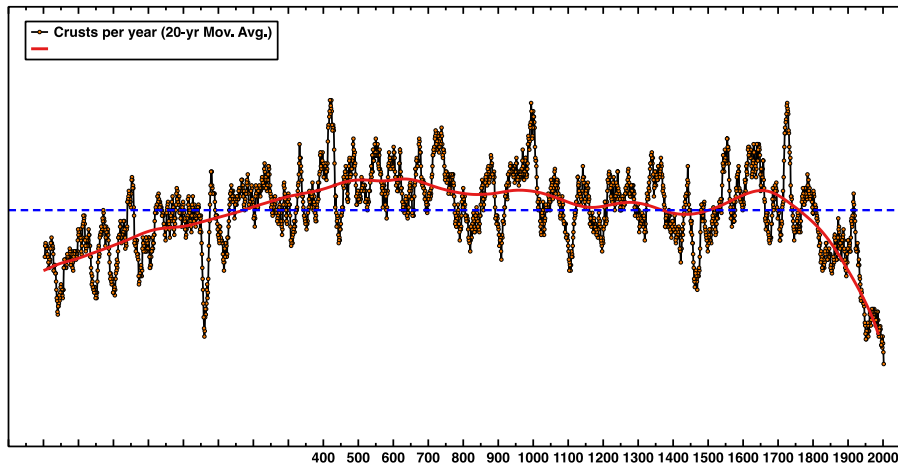




649  
 650  
 651  
 652  
 653  
 654  
 655

**Figure 14:** Density profiles measured in snow pits from five concurrent seasons at WAIS Divide (2008-2012). Each pit showed a high degree of sample-to-sample variability as measured densities were widely-spaced within the upper 2 meters of firm; estimated annual signals were still identifiable, however. Measurements yielded an overall average density of  $386.6 \pm 3.2 \text{ kg m}^{-3}$  for the upper 2 meters of firm across all 5 pits, with nearly identical linear trend-line slopes of  $\sim 0.4 \text{ kg m}^{-3} \text{ cm}^{-1}$  with depth.

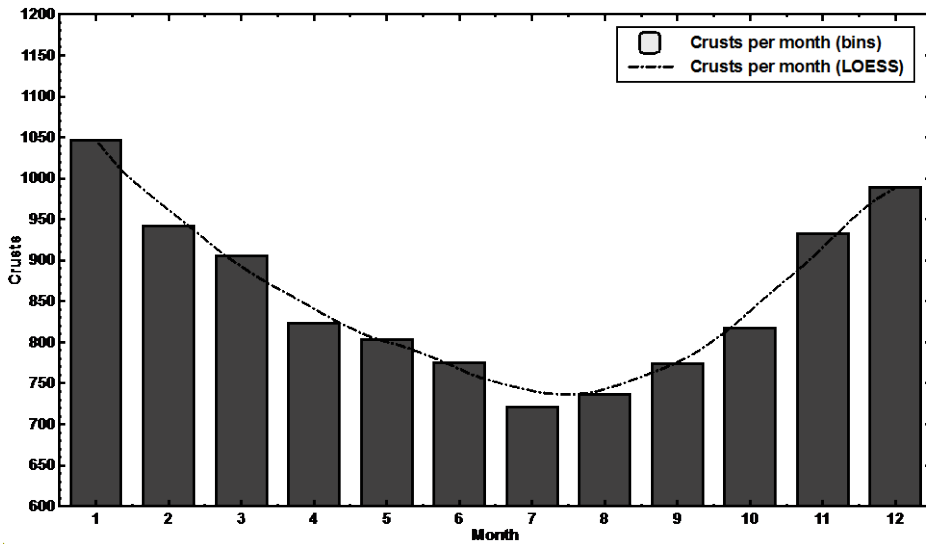
656 |



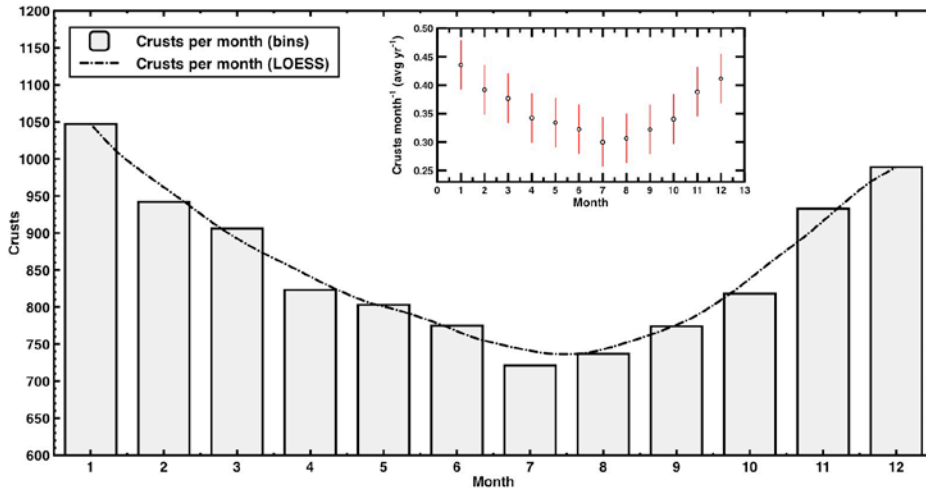
657

658

659 | **Figure 15:** History of crust occurrence (crusts year<sup>-1</sup>) in the bubbly-ice zone of the WDC06A  
660 core that we studied in detail (~120 – 577 m depth); ages (C.E.) are from the WD2014 depth-age  
661 scale). 10,268 unique crusts were documented in the core, for an average rate of  $4.3 \pm 2$  per year  
662 (dashed blue line). Data are shown as 20-yr moving averages for ease of view, with an added 1<sup>st</sup>-  
663 order LOESS smoothing trend-curve (200-yr bin-width). The sharp decline in crust prevalence  
664 after ~1750 C.E. may be due to observational biasing in the shallow firn.



665

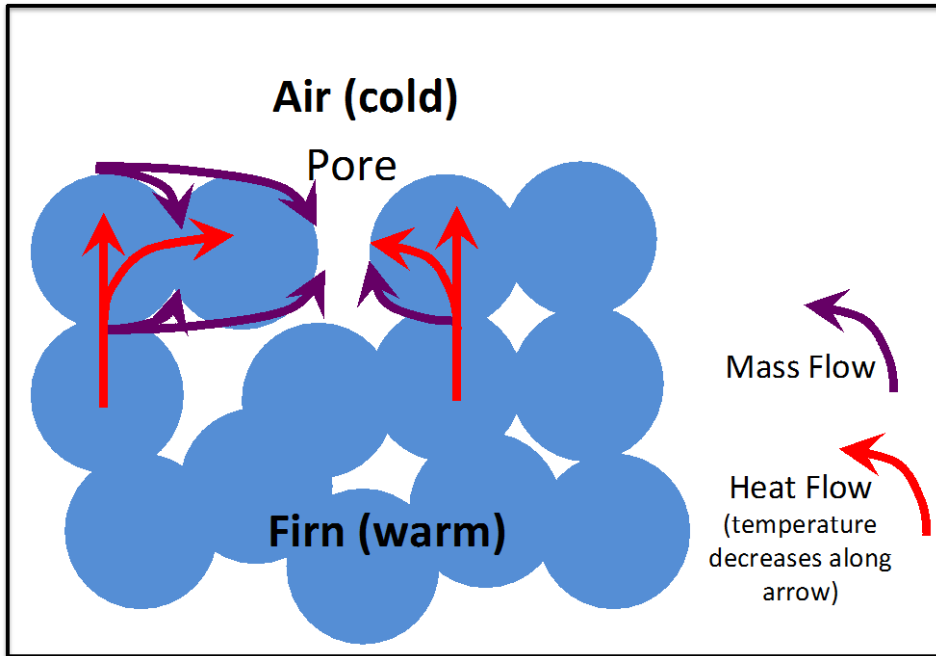


666

667

668 **Figure 163:** Crust distribution by month (1=January, 2=February,...12=December) based on  
 669 assumption that each summer pick in the WD2014 depth-age scale is January 1, and then  
 670 interpolating linearly. Crusts occur year-round but more commonly in summer accumulation. The  
 671 smoothed curve is a 1<sup>st</sup>-order LOESS trend curve (width = 2). [Data shown for 2400-yr record.](#)  
 672 [Inset shows average crusts per month \( \$\pm 1\sigma\$ \).](#)

Formatted: Font: Bold



673  
 674  
 675  
 676  
 677  
 678  
 679

**Figure 174:** Schematic illustrating possible mass and heat transports during during formation of a single-grain glazed crust, when the near-subsurface is warmer than the surface. Heat flow is primarily through the grain structure (blue), so pores (white) in the surface layer will be colder than interconnected grains, favoring mass transport from the grains to those pores, increasing density of the surface layer.

680 **Table 1:** Field observation table (see also Figs. 5, 6, 7, 8).

Field Season	Observation Window	Observation Duration	AWS	Other Instrumentation	Pit
2008-2009 <sup>1</sup>	12-Dec-2008 : 10-Jan-2009	~29 days	--	--	x
2009-2010 <sup>1</sup>	27-Dec-2009 : 25-Jan-2010	~29 days	W,H,T	--	x
2010-2011	20-Dec-2010 : 09-Jan-2011	~20 days	W,H,T	--	x
2011-2012 <sup>1</sup>	25-Dec-2011 : 04-Jan-2012	~12 days	W,H,T,I	Dual Li-Cor LI200 sensors	x
2012-2013 <sup>1</sup>	18-Dec-2012 : 30-Dec-2012	~12 days	W,H,T,I	Kipp-Zonen CNR2 sensor Shallow PRD strings <sup>2</sup>	x

W,H,T,I - Wind, Humidity, Temperature, Insolation

<sup>1</sup>Fegyveresi, 2015

<sup>2</sup>Muto et al., 2011

681